This is the Pre-Published Version.
C. Xiong, Z. Wang, X. Huang (2023) *Blow-off of Diffusion Flame by Air Vortex Ring*, **Experimental Thermal and Fluid Science**, 111059. https://doi.org/10.1016/j.expthermflusci.2023.111059

Blow-off of Diffusion Flame by Moving Air Vortex Ring

Caiyi Xiong[1,2], Zilong Wang[1], Xinyan Huang[1,*]

[1]*Research Centre for Fire Safety Engineering, Department of Building Environment and Energy Engineering, The Hong Kong Polytechnic University, Hong Kong*

[2]*School of Mechanical and Automotive Engineering, South China University of Technology, Guangzhou, Guangdong, China*

* Corresponding to xy.huang@polyu.edu.hk (X. Huang)

Abstract:

The blow-off is one of the typical flame extinction mechanisms, and such a principle has been widely used in firefighting when the water-based extinguisher is limited. This work explores the blow-off extinctions of different diffusion flames by air vortex ring. The vortex ring harnesses its kinetic energy within the fast-rotating vortex core, enabling the transmission of power over several meters to blow off a remote flame. The power required for vortex ring blow-off is found to be two to three orders of magnitude smaller than the power of the flame itself, demonstrating exceptional energy efficiency. It is observed that the poloidal flow (circulation) surrounding the vortex core can stretch the flame base to the critical state and then cause instantaneous extinction. To explain the vortex-induced blow-off limit, a critical Damköhler number that accounts for the competition between fuel gas flow and flame stretch was formulated. This work provides a fundamental understanding of the extinction mechanism by vortex ring, and it offers technical guidelines for using air as a flame extinguisher for remote firefighting within minimum energy input.

Keywords: *Buoyant flame; Extinction; Blow-off power; Firefighting; Air circulation; Flame stretch*

Graphic abstract

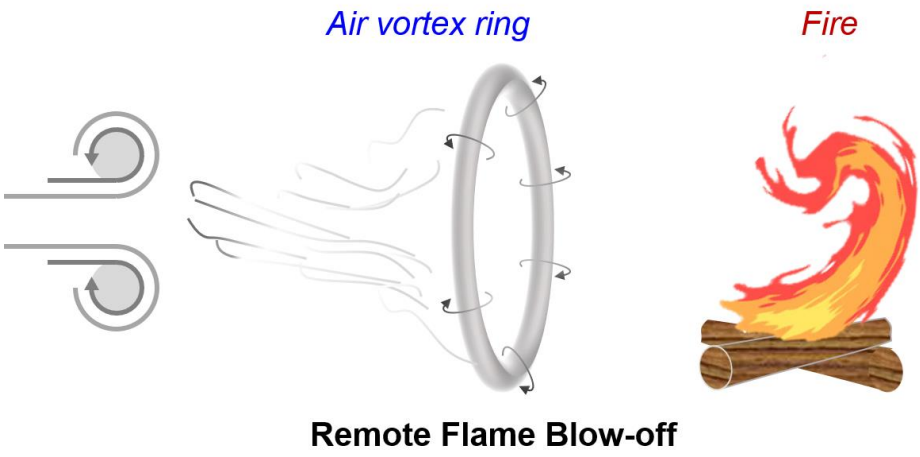

1. Introduction

The interaction between flame and wind has been an active research topic for over 70 years [1,2]. As the flame is essentially a gas-phase reaction between fuel gas and ambient oxygen, any change in the ambient flow can affect the flame dynamics and stability [3]. For example, increasing the airflow velocity can intensify the flame [4,5], deflect the fuel stream [6,7], create fire whirl [8], and even weaken the flame by cooling [9]. In particular, when the airflow speed is very large, the flame will be extinguished, also known as blow-off [10].

The flame blow-off has been widely studied in lab experiments under well-controlled external airflows or winds. Two mechanisms for flame blow-off are proposed, (1) within the flame sheet, the reduced flow residence time scale compared to the reaction time scale required for a continuous burning [10], and (2) in case of fire, a strong wind can also remove the solid fuel directly or reduce the gaseous fuel release from the solids by cooling [11], breaking the flame-fuel-supply cycle and leads to extinction [9,12]. Depending on the fuel type and flame characteristics, some critical blow-off velocity [13,14], stretch rate [15,16], or Damköhler number [10,17–19] can be used to quantify the flame blow-off limit.

Past studies have shown that even for small flames, the blow-off velocity can be very large, at least much larger than the flame-induced buoyancy flow [15]. In general, the larger the flame, the larger the buoyancy flow, and the larger wind speed is required for blow-off. The wind direction and fuel shape also matter. For instance, a 2 m/s wind is required to blow out the flame spreading on thin electrical wires [18], and a 3 m/s wind is needed to extinguish the flame concurrently spreading on a thin paper [20] or a wake flame hiding behind a plastic fuel [21]. In specific scenarios, a moderate rise in wind speed even cannot cause blow-off; instead, it amplifies the intensity of fire by increasing heat convection, as seen in pool fire cases [22]. However, the principle of blow-off flame extinction has still been adopted in firefighting, especially when water-based suppression is limited. For instance, the “leaf blower” is a common tool to fight wildfire by blowing away the leaves and twigs and blowing out the flame. However, this method involves a high safety risk, i.e., firefighters need to get close to the flame and blow it out in a short distance, because the fan-generated airflow diffuses shortly. Thus, the incapability of remote flame extinguishing limits the wider use of blow-off in flame suppression.

Vortex ring is a very special flow structure. It can be observed in life like the smoke ring produced by cigarette puffing (Fig. 1a) and the gas ring produced after airplanes (Fig. 1b). Such a structure mainly consists of an imaginary toroidal axis line, which is essentially a continuous distribution of different vortex centre cores combined with a certain mass of poloidal flows spinning around the core (Fig. 1c). As the poloidal flow isolates the core from the surrounding fluids, it continuously reduces the friction between them and avoids the dissipation of the core energy, which allows the vortex ring to typically travel several meters with little change in its rolling shape [23–25]. This characteristic lends itself to facilitating the remote suppression and blow-off of flames. In addition to the bulk poloidal motion, the ring core can concentrate energy and create another instant rotation, which effectively stretches the

flame sheet to promote the extinguishing process. Thus, compared to a steady wind blowing, a discrete air vortex ring may be more effective in remote flame blow-off with much lower energy consumption.

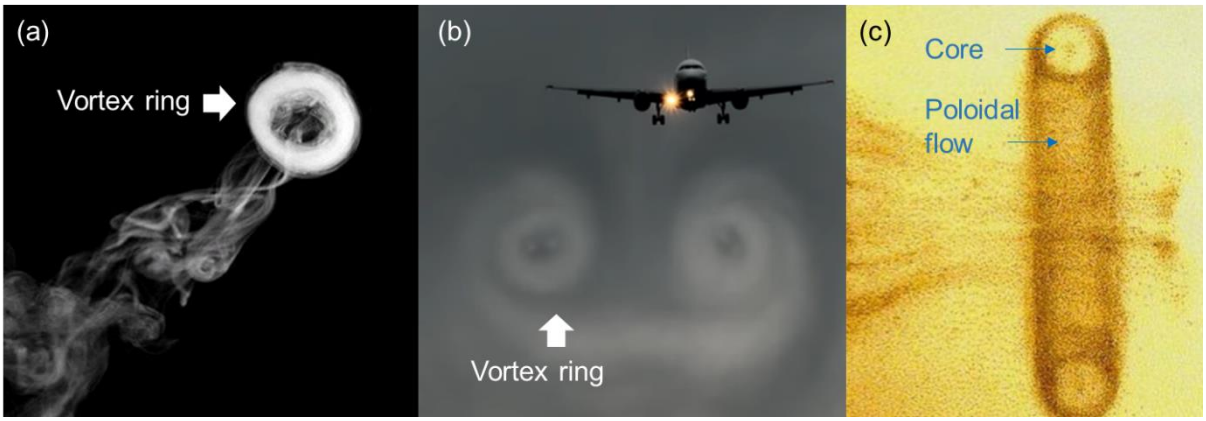

Fig. 1. (a) Smoke vortex ring [26], (b) gas vortex ring [27], and (c) sectional view of air vortex ring [28].

In the literature, although the vortex-flame interaction has been widely studied to better understand turbulent combustion [29–32], very limited works explore the use of air vortex ring to extinguish flames or suppress real fires. Akhmetov et al. [33] employed an air vortex ring produced by an explosion at the flame base to successfully extinguish a 27-m propane jet flame. Similarly, Giannuzzi et al. [34] achieved extinction by utilizing the same explosive-driven vortex ring, but from a horizontal direction. Nevertheless, it is evident that these explosion-based approaches are unsuitable for safe implementation in regular practice due to the associated production of hazardous shock waves. In short, the mechanisms and limits underlying flame blow-off by pure air vortex ring are still poorly understood, posing a big knowledge gap.

In this work, we carried out well-controlled lab experiments to investigate the blow-off of diffusion flames by air vortex ring. Different liquid fuel burners were used to produce typical buoyant diffusion flames of various power (or heat release rate, HRR). A membrane system was utilized to generate the target air vortex ring, which was then transmitted horizontally to affect the flame. The blow-off limit and extinguishing efficiency of the air vortex ring were examined. The critical flame behaviours prior to extinction were also analysed to gain insights into the underlying blow-off mechanism.

2. Experimental Method

2.1 Air vortex ring

Technically, the vortex ring structure is generated by impulsively expelling fluids from the vessel through a small orifice [33]. For safety reasons, the explosion-driven method is not applied here. Instead, a membrane-tube system was used to produce air vortex ring, seen in Fig. 2a. This system consists of a cylindrical tubular vortex generator made of plastic with an inner diameter of 400 mm, held by a steel frame to fix the tube axis 300 mm above the table surface. The air inside the tube will be the primary fluid to form the vortex ring.

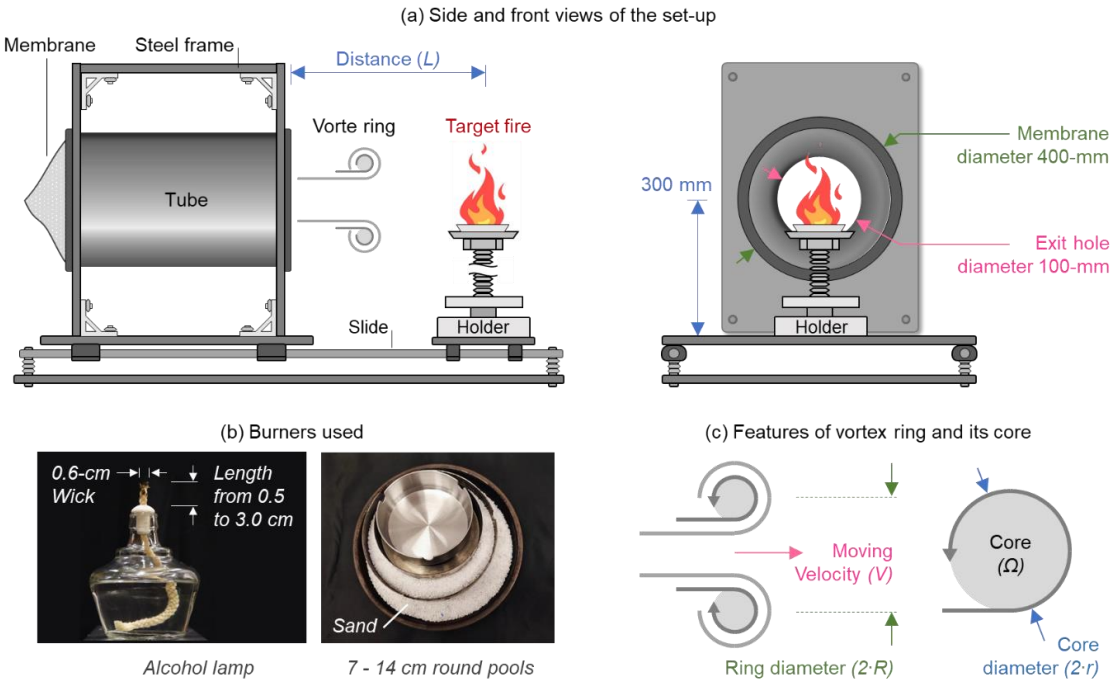

Fig. 2. (a) Side and front views of experimental set-up, (b) burners for different target flames, and (c) features of vortex ring and its core.

For the tubular vortex generator, one of its sides is covered by a piece of elastic polymer membrane (as the impulse source), and the other side is completely open in its centre with a 100 mm hole (as the exit). By stretching the membrane to the critical tension, a fixed amount of 0.5 L of air can be released from the exit hole within 1 s. Once entering the open space, the presence of axial velocity gradient will drive the columnar airflow to detach, curl, and roll up to form a single air vortex ring. By standardizing the vortex generation method and procedure, a relatively identical air vortex ring can be produced in each repeated test.

2.2 Target flames

Two types of flame are tested, (1) an ethanol burner with a cotton wick at various lengths, and (2) propanol pools of different sizes, see Fig. 2b. The ethanol burner is chosen because the small flame attached to the wick is stable and rarely has buoyancy-induced puffing. Also, the small-wick flame will not change by fuel regression in repeating tests. Thus, it is an ideal flame that can be entirely exposed to the air vortex ring to observe the detailed blow-off process and explore the mechanism. By varying the wick length (L_f) from 0.5 – 3.0 cm, the corresponding flame HRR changes within a small range of 119 - 177 W, as illustrated in Fig. 3a, determined by a standard method [35,36], i.e., by combining the measured mass loss from digital balance and the heat of combustion of ethanol $\Delta H_c = 29.7$ kJ/g.

To investigate how the air vortex ring extinguishes larger flames, different circular propanol pans with diameters of 3.5 – 14 cm are also tested. Note that the liquid-pool flame is not as well-controlled as the wick flame. To prevent the pool flame from moving with a regressing liquid level, all pans are pre-filled with sands soaked by propanol (Fig. 2b). A comparison of the flame HRRs of regular and

soaked liquid-pool flames in Fig. 3 shows their similarity, suggesting a negligible influence of soaked sands on fuel burning under current experimental conditions. All other key parameters of fuel, flame, and burner are given in Table 1.

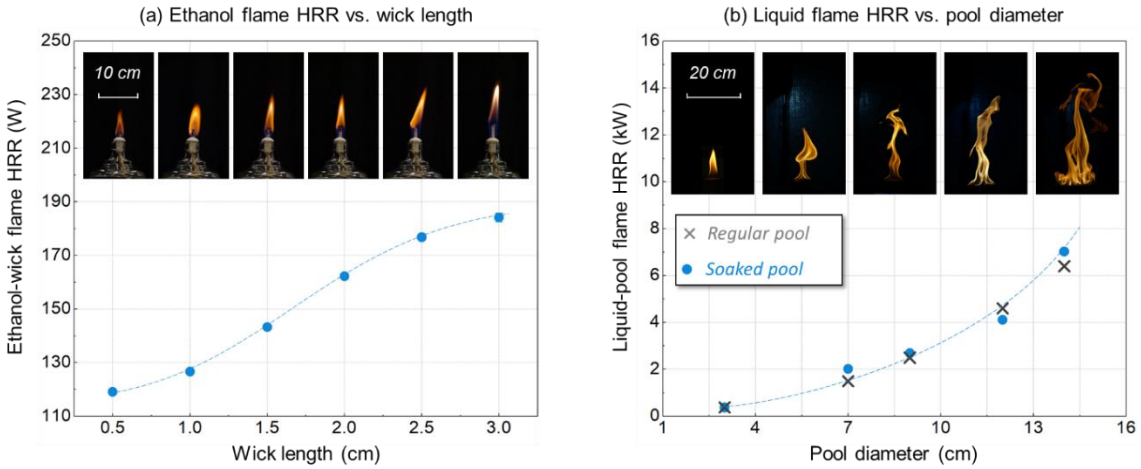

Fig. 3. (a) Variations of ethanol flame HRR at different wick lengths, and (b) a comparison of the flame HRR between regular and soaked liquid pools; where the heats of combustion of ethanol and propanol use 29.7 kJ/g and 33.6 kJ/g, respectively.

2.3 Experiment procedure

During the experiments, the tubular vortex generator is placed in a horizontal direction to produce transverse air vortex rings one by one. A large test room with a size of 8 m (length) × 5 m (width) and 3.7 m (height) allows for free propagation of the air vortex ring in a quiescent environment. Before the experiment, the burner was placed in a specific position, and a propane torch was used to ignite all fuels from the top. The target flames are tested at two heights, levelling with the upper and lower boundaries of the exit hole, so only the top and bottom of the air vortex ring can affect the flames. To reach a stable burning, all flames were free to develop for at least 5 s (small-wick flame) and 20 s (liquid-pool flame).

Table 1. Parameters for the fuel, flame, and burner used in the current work.

Fuel and burner	**Wick length (L_f) [cm]**	**Pool diameter (D) [cm]**	**Flame height [cm]**	**HRR [W]**
Ethanol and cotton-wick burner	0.5	N/A	3.7	119
	1.0		4.0	127
	1.5		4.4	143
	2.0		5.0	162
	2.5		7.1	177
	3.0		9.2	184
Propanol and soaked circular pool	N/A	3.5	10.4	370
		7.0	20.5	2017
		9.0	27.0	2688
		12.0	32.0	4109
		14.0	45.0	7021

When the air vortex ring moves in the open space, its intensity decreases gradually along the propagation path. The distance between the hole exit and flame can vary from 0 – 4 m by moving on the bottom slider. The extinction limits of different flames can be estimated based on measuring the critical blow-off distance. A successful blow-off is defined as a flame that weakens rapidly upon encountering the vortex ring, disappears thereafter, and does not reignite on its own.

Identifying the vortex ring features is still required before extinguishing trials. However, the air vortex exhibits transparency and inhomogeneity in all dimensions. To improve visualization, a small amount of white smoke (produced by FLASH FM-2000) is filled into the tube during preliminary tests to produce a smoke ring. Additionally, a planar laser is applied along the vortex path and enhance measurement clarity. Critical flame behaviours leading up to extinction are monitored using a high-speed camera. To estimate the probability of extinction and mitigate random test errors, each blow-off trial is repeated 30 times.

3. Results and discussion

3.1 The air vortex ring features

Fig. 4a illustrates the evolution of the ring structure over a short propagation distance as an example (also see Video S1). From the videos, three parameters closely related to the ring propagation and evolution, including the ring translational speed V, ring radius R, and core radius r (defined in Fig. 1c), can be measured. Note that these measurements can only be carried out up to a 4-m travel distance before the smoke vortex dissipates and becomes blurred.

Fig. 4(b-e) summarize all the measuring parameters versus the ring propagation distance. The vortex ring continues to develop in the open space for about 0.5 m after leaving the tube, as revealed by the sharp increase in the ring translational velocity in Fig. 4b. During this developing stage, the ring detaches from its feeding jet and expands its volume (also see Video S2). Thus, only the fully developed air vortex rings propagating greater than 0.5 m are used to blow out the flames.

According to the vortex ring theory [37], the ratio of the ring radius to the core radius, as measured in Fig. 4e, can define the thin ring (ratio < 1) and thick ring (ratio > 1). Fig. 4a shows that the ring continues to expand as the core shrinks during free propagation. Thus, the radius ratio is significantly smaller than 1 for the developed rings, evidenced by Fig. 4e, leading to the available use of the thin-core vortex ring theory [24,37] that assumes the core radius to be infinitesimal compared to the ring size. Note that for intuitive calculations, all equations have been transformed by moving the ring parameters to the right-hand sides.

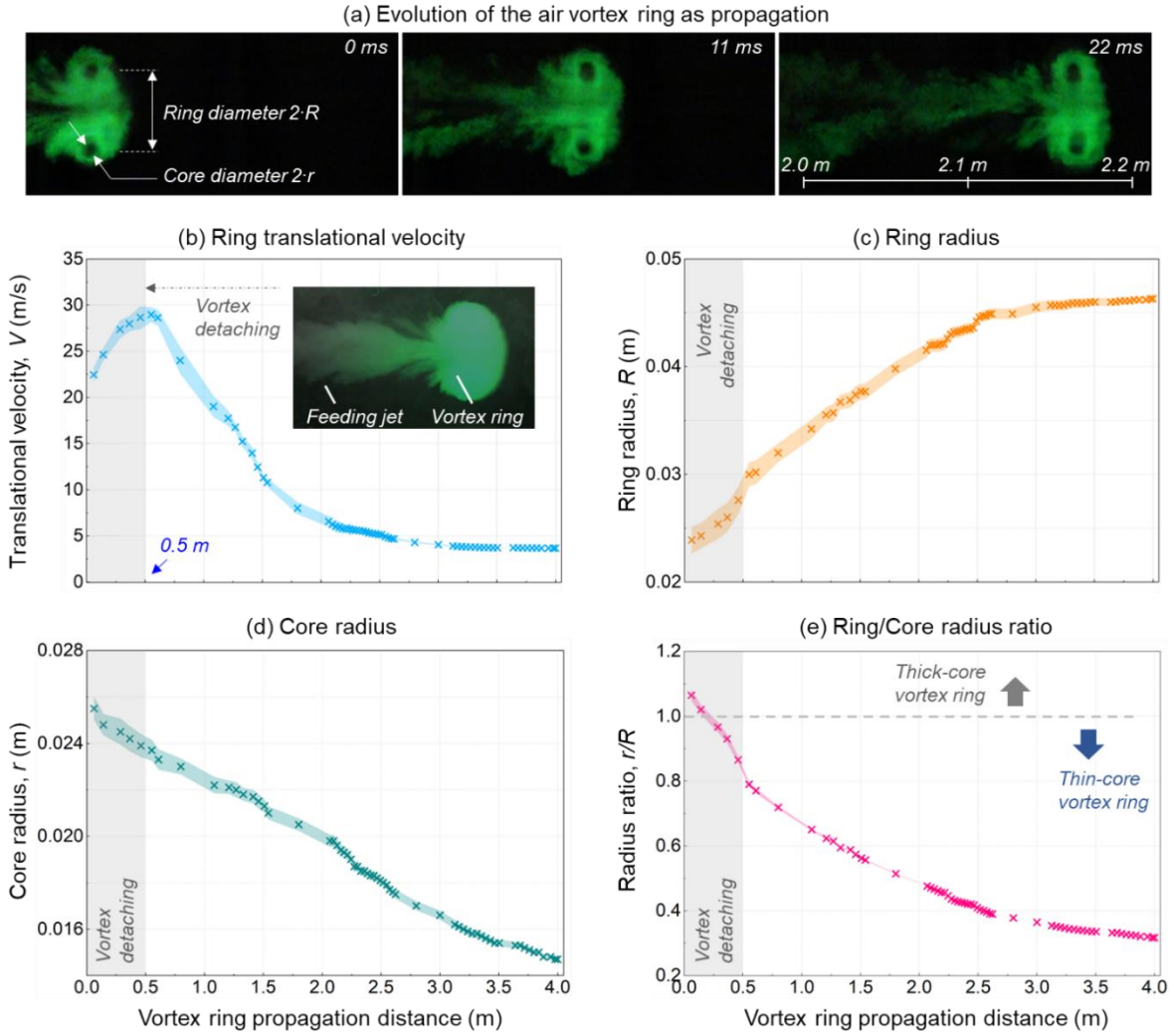

Fig. 4. (a) Evolution of the ring structure, and variations of (b) ring translational speed V, (c) ring radius R, (d) core radius r, and (d) ring/core radius ratio over the path (see Videos S1 and S2).

For the original equations, please refer to [24,37].

$$\Omega = \frac{4VR}{r^2} \cdot \left(ln\frac{8R}{r} - \frac{1}{4} \right)^{-1} \tag{1}$$

$$\Gamma = 4\pi VR \cdot \left(ln\frac{8R}{r} - \frac{1}{4} \right)^{-1} \tag{2}$$

$$I = 4\rho\pi^2 VR^3 \cdot \left(ln\frac{8R}{r} - \frac{1}{4} \right)^{-1} \tag{3}$$

$$E = 8\rho\pi^2 V^2 R^3 \cdot \left(ln\frac{8R}{r} - \frac{1}{4} \right)^{-2} \cdot \left(ln\frac{8R}{r} - \frac{7}{4} \right) \tag{4}$$

Here, Ω and Γ are the vorticity and circulation distributions over the vortex core, while I and E are the hydrodynamic impulse and kinetic energy concentrated by the core. As the right-hand sides of Eqs. (1-4) exclusively include the ring propagation and evolution parameters in Fig. 4, their solutions can

be calculated directly and summarized in Fig. 5. For validation, the ring vorticity Ω was additionally determined through analysing videos, as illustrated in Fig. 5a. The similarity between the measured and predicted values serves as a confirmation of the above equations.

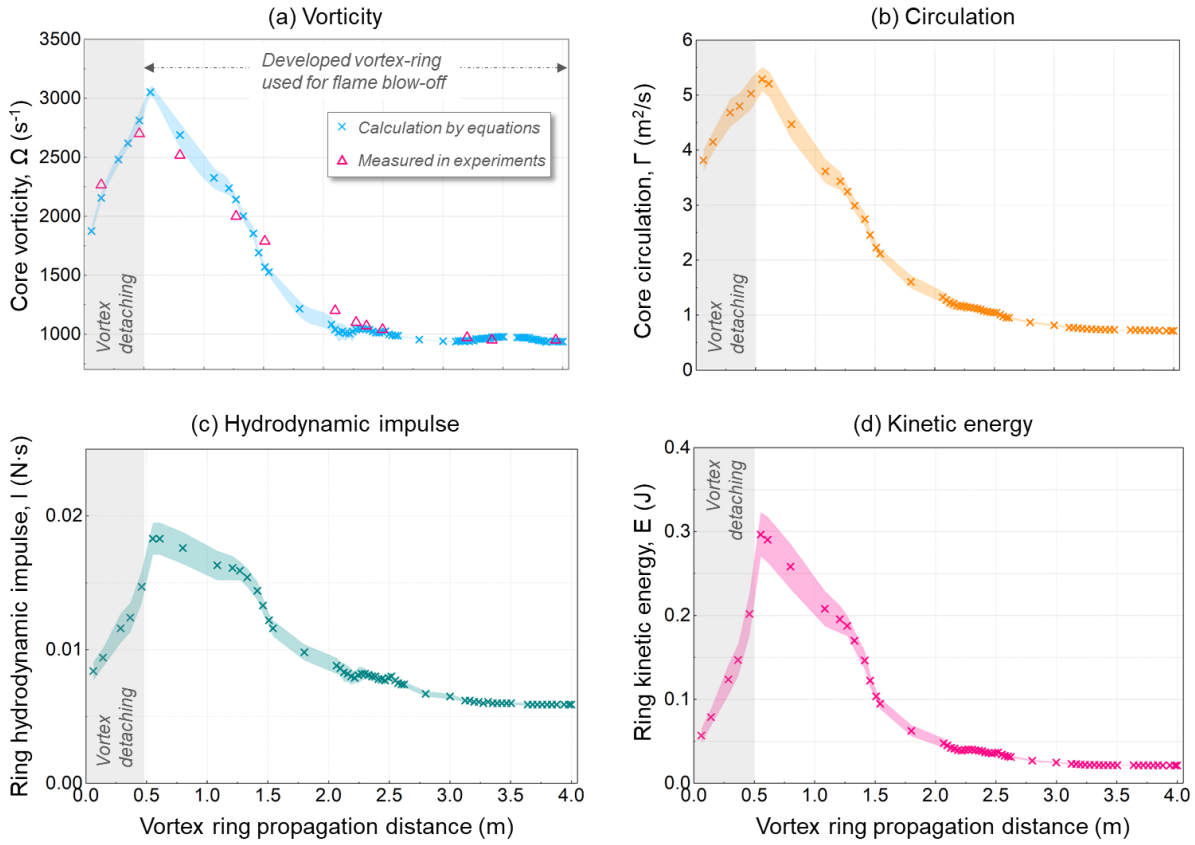

Fig. 5. Variations of the air vortex ring's (a) vorticity Ω, (b) circulation Γ, (c) hydrodynamic impulse I, and (d) kinetic energy E over the propagation path.

3.2 Flame blow-off process by air vortex ring

Fig. 6 shows a typical blow-off process of an ethanol flame with a 2-mm wick (162 W) by an air vortex ring at a 2-m propagation distance. Two representative scenarios are examined, where the flame is blown off by (a) the top part of the vortex ring (anti-clockwise rotating ring) and (b) the bottom part of the vortex ring (clockwise rotating ring), respectively. In both cases, the extinction duration is very fast, around 20 ms. Also, the flame behaviour shows remarkable similarities, as it is initially deflected from the fuel source by the vortex and subsequently undergoes twisting motions along the spinning flow surrounding the core (see Video S3). As seen, extinction occurs immediately after the flame is completely "peeled off" from the wick. Note that normal wind can also cause the same extinction, but a ~ 5 m/s fan [38] combined with a 2-m wind tunnel is required to initiate this remote blowing, as the airflow is easily dissipated and takes at least a few seconds to cool the burner and extinguish it.

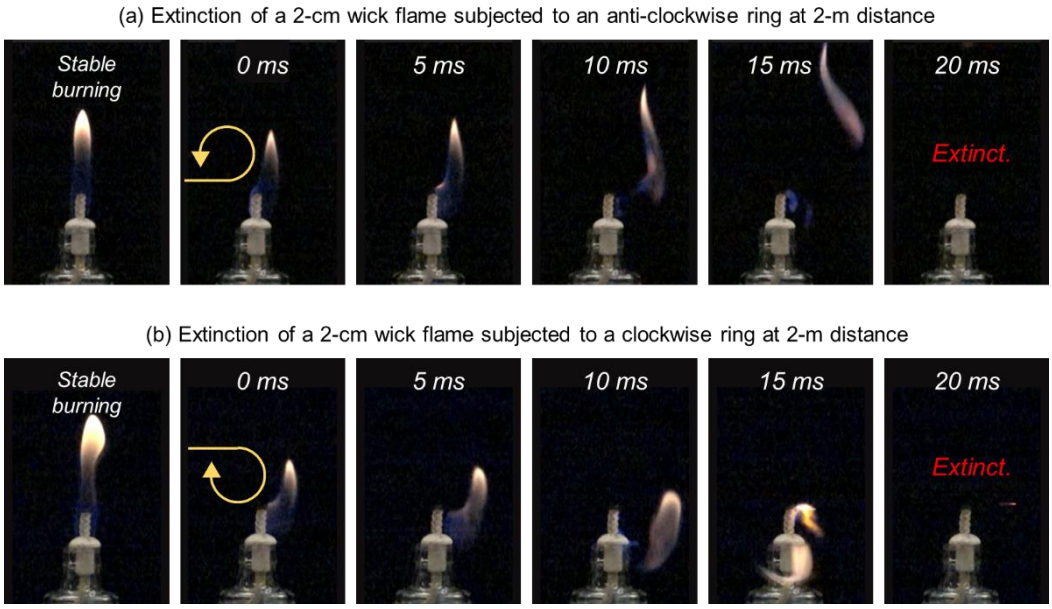

Fig. 6. Extinctions of a 2-cm wick ethanol flame by (a) the top and (b) bottom parts of the vortex ring at a 2-m propagation distance (see Video S3).

A comparable blow-off process can be observed when the vortex ring affects the liquid-pool flame. Preliminary tests have shown that the extinction of the liquid-pool flame only occurs when the vortex ring affects the flame base (bottom). Fig. 7a illustrates a successful blow-off of a 9-cm pool flame (2688 W) by the same air vortex ring at a 2-m distance (also see Video S4).

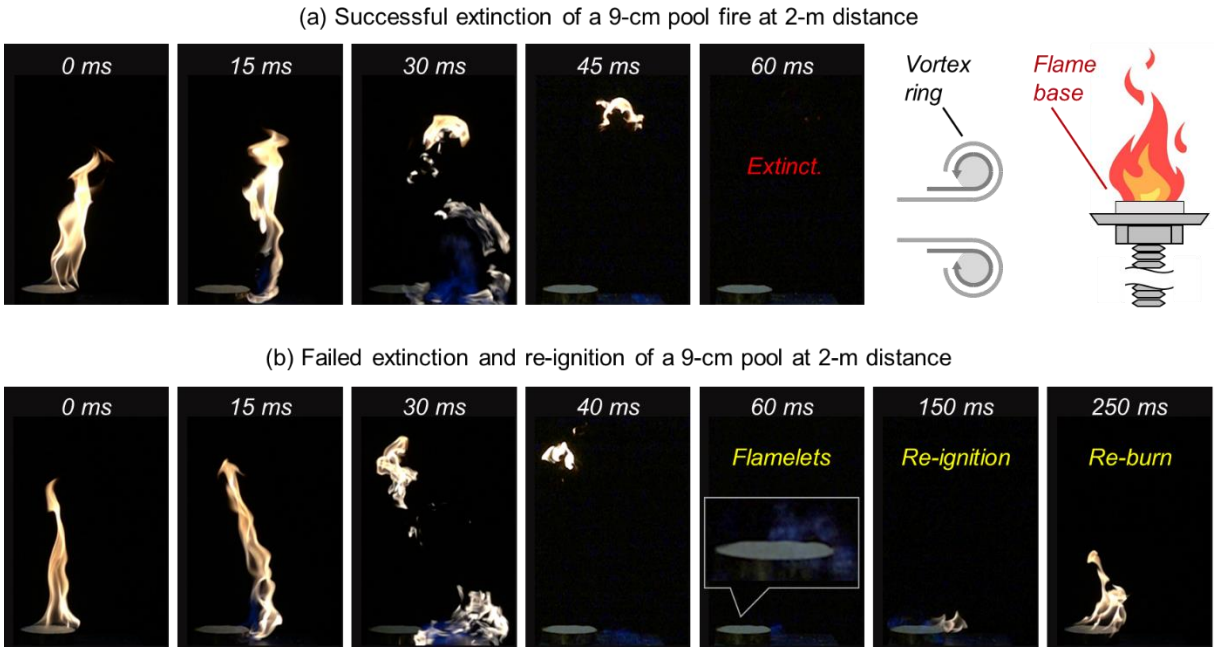

Fig. 7. (a) Successful and (b) failed extinctions of a 9-cm pool flame by air vortex ring at a 2-m propagation distance (see Video S4).

Despite the pool fire having a power (or HRR) more than 10 times greater than the wick flame, their responding behaviours are similar. Both flames are deflected and stretched by the vortex ring until

they weaken and disappear. One distinction is that the blow-off duration for liquid-pool flame increases (about 60 ms). Another notable difference is that the flame extinction does not occur in every attempt with the pool flames, indicating that a flame with a higher HRR is more challenging to extinguish.

Occasionally, as depicted in the 60-ms snapshot shown in Fig. 7b, weak blue flamelets can persist at the pool edge, despite the majority of the yellow flame vanishing as the vortex ring propagates through (also see Video S4). Subsequently, these weak flames gradually intensify, turning yellow again and re-igniting the fuel pool, resulting in a failed blow-off process. On the ground of this, it is possible to quantitatively determine the blow-off limits as a function of vortex kinetic parameters by varying the flame HRR and the propagation distance of the vortex ring.

3.3 Flame blow-off limit of air vortex ring

A series of repeated experiments are conducted to examine the blow-off limits of the air vortex ring. Various small-wick flames and pool flames are tested at different distances along the path of ring propagation. Considering the significant uncertainties associated with past studies on spotting ignition and extinction [39,40], the probability of flame extinction (P_{ex}) can be calculated in repeated tests as:

$$P_{ex} = \frac{N_{ex}}{N_{tot}} \times 100\% \tag{5}$$

where N_{ex} is the number of successful extinction and $N_{tot} = 30$ is the total number of repetitions.

By defining the probability of 100% as the critical value, the critical propagation distance at which the air vortex ring can absolutely cause blow-off can be determined in each case. In other words, above this boundary, flame extinction is not guaranteed. To accurately determine the critical distance, all flames are incrementally moved upstream towards the vortex source (hole exit) within the potential region, with steps of 0.1 m, until a 100% probability of extinction is achieved. Fig. 8a shows the blow-off probabilities for different wick flames as a function of flame HRR. The most prominent feature is the decrease in extinction probability as both the ring propagation distance and the flame HRR increase. This trend is similarly observed for large propanol flames in Fig. 8b.

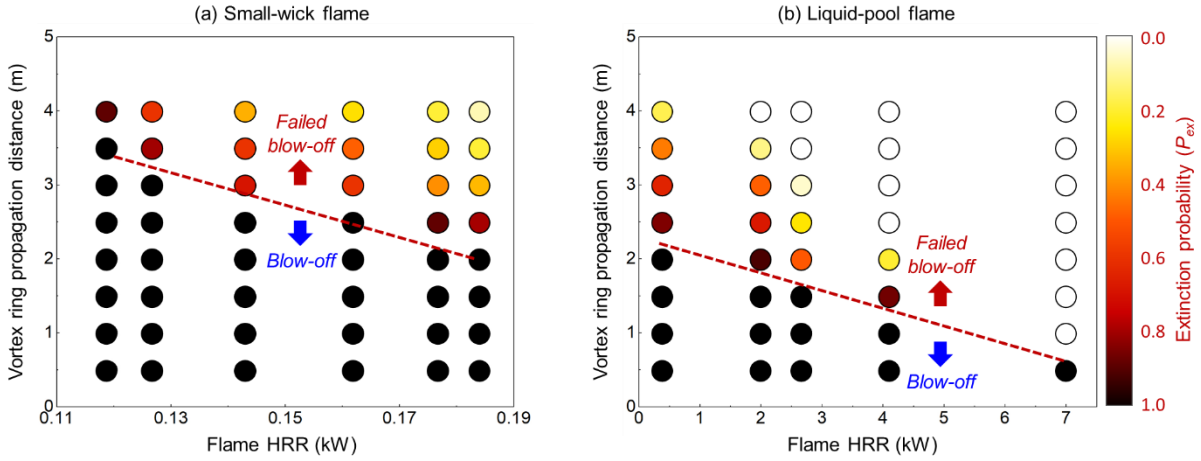

Fig. 8. Extinction probabilities of (a) small-wick flame and (b) liquid-pool flame by air vortex ring at different distances; the critical distance dash line is determined by P_{ex} = 100%.

By quantifying the critical distance of flame blow-off, the critical parameters (vorticity, circulation, hydrodynamic impulse, and kinetic energy) required for the air vortex ring can be determined, as summarized in Fig. 9. Note that these parameters are not obtained independently, but are calculated by coupling based on underlying thin-core vortex theory [24]. Thus, all the vortex-ring parameters in Fig. 9 exhibit a positive correlation with the flame HRR. In other words, all these parameters have the potential to serve as indicators of the flame blow-off limit.

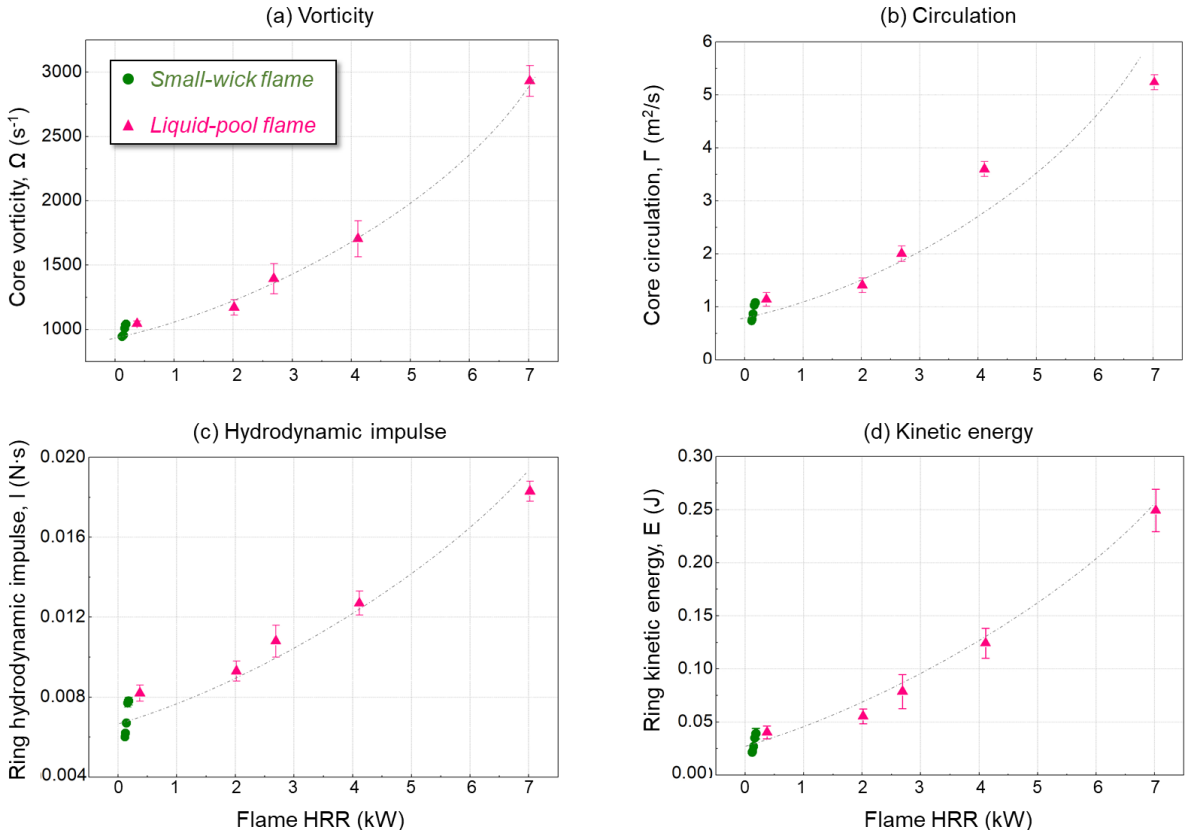

Fig. 9. Critical states of air vortex ring at blow-off limits, including (a) vorticity, (b) circulation, (c) hydrodynamic impulse, and (d) kinetic energy.

3.4 Flame blow-off mechanism by air vortex ring

To explain the blow-off phenomenon, thoughts turn first to the preferential diffusion by the Lewis number effect [41,42], where the fuel gas burning velocity may become too small compared to the local flow velocity due to the circulation-induced flame stretch. However, the current circulation is caused by external air vortex ring, leading to the diffusion thickness of gas fuel and air into the reaction zone to be governed by vortex boundary rather than combustion consumption. Also, the current target flames are supported by condensed liquids rather than gas fuels. Thus, some other methods to connect the vortex flowing pattern with liquid burning evaporation are expected.

Due to the occasional occurrence of re-ignition, using the Damköhler (Da) number to describe the blow-off of diffusion flame can be a more suitable indicator [10]. Given that extinction is guaranteed only if the flame base is completely detached and blown off during the impact of vortex ring, a critical

Da number is proposed to compare the local gas flow residence time (t_{re}) near the fuel source with the fuel ignition delay time (t_{ig}) over the burner surface as

$$Da = \frac{t_{re}}{t_{ig}} \tag{6}$$

For the fuel residence time t_{re}, since the vortex ring still maintains a certain travel speed and moves forward during fast rotation, a processing method similar to the wind-blowing situation is adopted, i.e., achieved by the ratio of the burner characteristic size over the vortex ring translational speed as

$$t_{re} = \frac{U}{D} \tag{7}$$

where D in pool fire cases stands for the pan diameter, and in wick-flame cases is wick diameter and fixed at 0.6 cm (see Fig. 2b).

To maintain a flame under external disturbance, the fuel gas near the source burner should be able to be re-ignited or piloted by the near flamelets. In other words, the fuel gas needs to be sufficiently heated to evaporate and flow into the air, which requires a duration of t_{flow}. Then, there is another time scale for the fuel vapor to mix with air and reach the flammable limit, referred to as t_{mix}. Following the ignition or pilot, the gas mixture requires a further time interval, denoted as t_{chem}, for chemical reactions to produce a flame. In this way, the ignition delay can be estimated as:

$$t_{ig} = t_{flow} + t_{mix} + t_{chem} \tag{8}$$

In general, the gas-phase chemistry exhibits rapid kinetics [43], so the ignition delay is primarily governed by fuel evaporation flowing and gas-phase mixing. To estimate the relevant timescales, it is crucial to consider a boundary layer induced by the vortical flow above the burner surface. However, assessing the hydrodynamic boundary directly poses challenges due to the intricate dynamics of near-wall vortices [44]. Here, we borrowed the concept from near-wall turbulence and scaled it to estimate the thickness of the hydrodynamic boundary, denoted as δ, resembling that of the turbulent vortex sheet resulting from the distortion by wall perturbation [45] as

$$\delta = \begin{cases} \frac{1}{2}\left[\frac{(R-L_f)(r-L_f)^2 v}{\Gamma}\right]^{1/3} & [small-wick\ flame] \\ \frac{1}{2}\left(\frac{Rr^2 v}{\Gamma}\right)^{1/3} & [liquid-pool\ flame] \end{cases} \tag{9}$$

where v = 84.9 × 10^{-6} m^2/s is the air viscosity [46] at 800 K (flame-air average temperature), L_f is the wick length, and $(R - L_f)$ and $(r - L_f)$ represent the impacts of wick geometry on the integrity of the core and ring structures. Based on Eq. (8), the fuel flowing time can be estimated as

$$t_{flow} = \frac{\delta}{v_f} \tag{10}$$

where v_f should be the evaporation-induced fuel exit velocity. According to [47,48], v_f is obtained as

$$v_f = \begin{cases} \dfrac{4HRR \cdot T_b}{\rho_{g0}\rho_g T_o \Delta H_c \left(\pi D^2 + \pi D L_f\right)} & [small - wick\ flame] \\ \dfrac{4HRR \cdot T_b}{\rho_{g0} T_o \Delta H_c \pi D^2} & [liquid - pool\ flame] \end{cases} \quad (11)$$

Here, T_b is the fuel boiling temperature (351 K for ethanol and 355 K for propanol), T_o is the bulk fuel temperature (all taken as around 338 K following [49]), and ρ_{g0} is the evaporated gas density at T_o (1.63 kg/m^3 for ethanol and 1.42 kg/m^3 for propanol). The only difference between the two equations in Eq. (10) is the fuel exit surface, where the fuel can only exit from the top surface of the round pool, but can exit from all sides and top of the cylindrical wick. As a result, t_{flow} is calculated as

$$t_{flow} = \begin{cases} \dfrac{1}{2}\left[\dfrac{\left(R - L_f\right)\left(r - L_f\right)^2 v}{\Gamma}\right]^{1/3} \dfrac{\rho_{g0}\rho_g T_o \Delta H \left(\pi D^2 + \pi D L_f\right)}{4HRR \cdot T_b} & [small - wick\ flame] \\ \dfrac{1}{2}\left(\dfrac{Rr^2 v}{\Gamma}\right)^{1/3} \dfrac{\rho_{g0}\rho_g T_o \Delta H \pi D^2}{4HRR \cdot T_b} & [liquid - pool\ flame] \end{cases} \quad (12)$$

On the other hand, by assuming that the concentration boundary has the same thickness as the hydrodynamics boundary layer (in the case of a unit Schmidt number [43]), the fuel mixing time can be determined using the diffusion law [36] as:

$$t_{mix} = \frac{\delta^2}{\alpha} = \begin{cases} \dfrac{1}{4\alpha}\left[\dfrac{\left(R - L_f\right)\left(r - L_f\right)^2 v}{\Gamma}\right]^{2/3} & [small - wick\ flame] \\ \dfrac{1}{4\alpha}\left(\dfrac{Rr^2 v}{\Gamma}\right)^{2/3} & [liquid - pool\ flame] \end{cases} \quad (13)$$

where α = 120 × 10^{-6} m^2/s is the diffusivity of air mixture at 800 K [50].

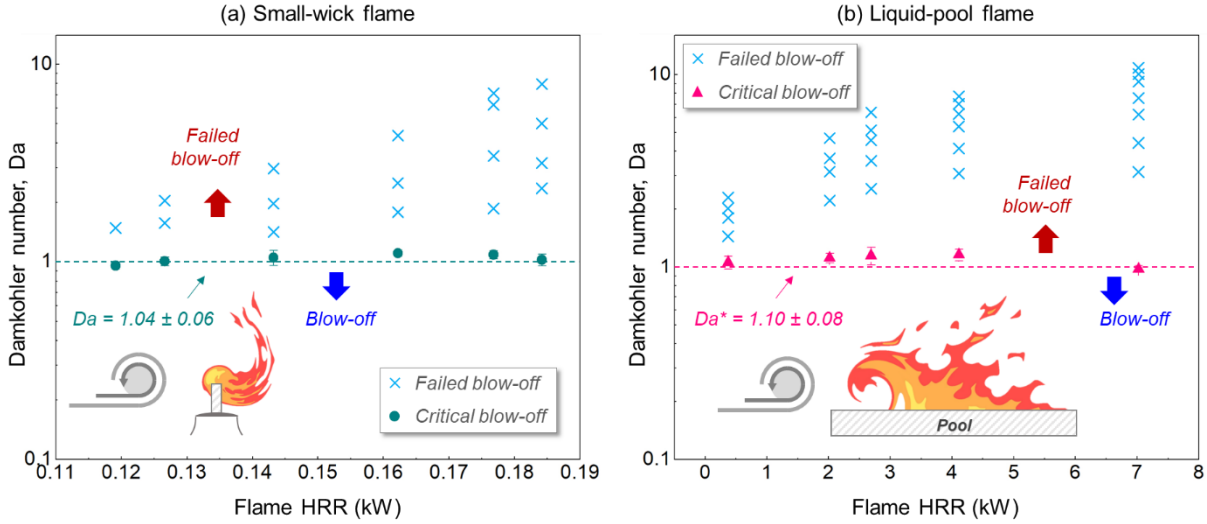

Fig. 10. Solutions of Da number for (a) small-wick flame and (b) liquid-pool flame at extinction limits, where the Da criteria for failed blow-off cases were also given.

Combining Eqs. 6-12 yields a nearly constant critical Da number (approximately 1.0 under the current parameter assumptions) for all blow-off limits, irrespective of the fuel and burner used, as seen

in Fig. 10. This suggests that the proposed Da criterion has the potential for broader application in predicting blow-off extinction by air vortex ring. For a group of flame and vortex ring with $Da > 1.0$, re-ignition may occur, allowing the flame to continue burning, while if the vortex can ensure $Da < 1.0$, an instant flame blow-off is expected. The Da criterion also highlights that, for a given air vortex ring, its blow-off limit depends not only on vortex dynamics, fuel properties and gas-phase diffusion, but also on the relative position of the ring structure and the target burner. Details of this phenomenon will be the subject of future study.

3.5 Blow-off power efficiency of air vortex ring

It is also worth noting that blow-off by an air vortex ring does not necessitate continuous blowing or the presence of multiple vortices. Instead, it only requires an instant energy release to significantly stretch the flame. The kinetic energy of the vortex ring originates from the impulse energy of a stretched membrane through a piston-like compression, so there is a high energy conversion efficiency during the generation process of the air vortex ring.

Re-examining Fig. 5d, it is seen the decay of the ring kinetic energy is not rapid, as it decreases from 0.3 to 0.02 J while propagating from 0.5 to 4.0 m. However, despite such a modest energy input, the resulting vortex ring proves to be sufficiently robust to extinguish distant flames with a wide range of HRR from 119 to 7021 W along its path. This observation highlights that although generating an air vortex ring requires minimal power, it possesses the capability to extinguish flames with significant power outputs, which deserves further quantification.

By assuming that all the energy within the vortex core is released for flame blow-off, a blow-off efficiency index (β) for a single vortex ring can be defined as the ratio of flame power (P_{fl} or HRR) to the critical power of the air vortex ring (P_v) as

$$\beta = \frac{P_{fl}}{P_v} \tag{14}$$

where P_v can be estimated as a complete release of the vortex kinetic energy over the extinction duration (25 ms for wick-flames and 60 ms for pool fires, following Figs. 6-7). A comparison of the flame powers to the critical power of air vortex ring required for 100% extinction is given in Fig. 11a. It is seen that the ring powers are two to three orders of magnitude lower than those of the target flames, which supports a vortex ring with less than 1% of the flame power is capable of inducing blow-off.

The value of β is further given in Fig. 11b, which serves as a characterization of the air vortex ring capability to extinguish flames with unit energy along its path. As the ring propagates and weakens, the blow-off index decreases but remains greater than 10^2. Such a large value of β, albeit a rough estimation, indicates the remarkably high energy efficiency of a single air vortex ring in causing remote extinction. In comparison, the conventional "leaf blower" requires close contact between the wind generator and the flame, as mechanically generated wind, despite its strength, dissipates quickly.

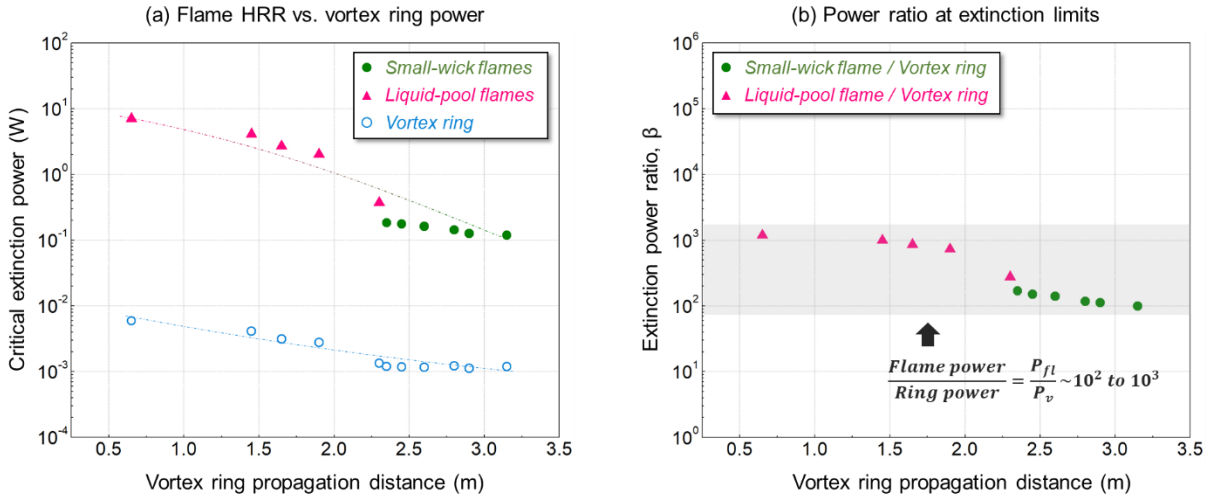

Fig. 11. (a) A comparison of the critical powers of flame and air vortex ring, and (b) the flame/ring power ratio at extinction limits.

It is expected that the vortex-ring flame blow-off method has a wide range of applications. For example, a vortex generator can be carried by a UAV or firefighting robot to extinguish the flame in a hazardous area. In the microgravity spacecraft environment, vortex ring can be more effective in terms of fire suppression because it can propagate longer with less disturbance of buoyancy. This blow-off method is still a new concept for potential firefighting application, and it can be combined with conventional fire suppression agents like water mist or inert gas, but each worth more investigation.

4. Conclusions

This work investigates the remote blow-off of diffusion flames by an air vortex ring. To generate the vortex ring, a membrane-tube system is employed, allowing for propagation distances of up to 4 m and subsequent extinguishment of the diffusion flame. The power or HRR of tested diffusion flames varies from 119 to 7021 W. Through extensive repeated testing, the probability of extinction for the diffusion flames is determined at different ring propagation distances.

Due to the unique structure, the air vortex ring can concentrate most kinetic energy within its core and maintain its transmission over considerable distances with minimal energy dissipation. The vortex ring first consistently detaches the flame sheet from the fuel surface, then deforms and rotates the flame along its spinning pattern of the vortex core, and eventually blow out the flame. An extinction criterion based on a critical Damköhler number around 1.0, coupling the fuel, flame, burner and vortex parameters, is formulated to reveal the competition between fuel evaporation release and flame stretch near the extinction limit. The air vortex ring with less than 1% of the flame power is found to be sufficient to blow off the flame, demonstrating exceptional energy efficiency.

This work provides some fundamental understanding of the extinction mechanism behind the air vortex ring, and it broadens the conventional firefighting methods and offers the design of an energy-saving remote blow-off technique by just using normal air. The combination of such technology with

other flame-suppressing agents like inert gas and water mist can be more promising. Future research is still required on the influence of vortex power, ring orientation, and generation frequency to seek deeper insights into the blow-off mechanisms and practices of air vortex ring.

CRediT authorship contribution statement

Caiyi Xiong: Investigation, Methodology, Formal analysis, Writing - original draft. **Zilong Wang**: Investigation, Resourcing. **Xinyan Huang**: Conceptualization, Formal analysis, Methodology, Writing - review & editing, Supervision.

Declaration of Competing Interest

The authors declare that there is no conflict of interest.

Acknowledgements

This work is funded by National Natural Science Foundation of China (NSFC grant No. 52006185), and the Hong Kong Research Grants Council Theme-based Research Scheme (T22-505/19-N).

References

[1] Wohl K, Kapp NM, Gazley C. The stability of open flames. *Proceedings of Combustion Institute* 1949;3:3–21.
[2] Williams FA. A review of flame extinction. *Fire Safety Journal* 1981;3:163–75.
[3] Pitts WM. Wind effects on fires. *Progress in Energy and Combustion Science* 1991;17:83–134.
[4] Tang F, Li LJ, Zhu KJ, Qiu ZW, Tao CF. Experimental study and global correlation on burning rates and flame tilt characteristics of acetone pool fires under cross air flow. *International Journal of Heat and Mass Transfer* 2015;87:369–75.
[5] Eftekharian E, Ghodrat M, He Y, Ong RH, Kwok KCS, Zhao M. Numerical analysis of wind velocity effects on fire-wind enhancement. *International Journal of Heat and Fluid Flow* 2019;80:108471.
[6] Tsuji H. Counterflow diffusion flames. *Progress in Energy and Combustion Science* 1982;8:93–119.
[7] Xiong C, Wang Z, Huang X. Acoustic flame extinction by the sound wave or speaker-induced wind? *Fire Safety Journal* 2021:103479.
[8] Tohidi A, Gollner MJ, Xiao H. Fire Whirls. *Annual Review of Fluid Mechanics* 2018;50:annurev-fluid-122316-045209.
[9] Fernandez-Pello a. C, Hirano T. Controlling mechanisms of flame spread. *Combustion Science and Technology* 1983;32:1–31.
[10] Williams FA. Progress in knowledge of flamelet structure and extinction. *Progress in Energy and Combustion Science* 2000;26:657–82.
[11] Lin S, Chow TH, Huang X. Smoldering propagation and blow-off on consolidated fuel under external airflow. *Combustion and Flame* 2021;234:111685.
[12] Huang X, Gao J. A review of near-limit opposed fire spread. *Fire Safety Journal* 2021;120:103141.
[13] Hu L. A review of physics and correlations of pool fire behaviour in wind and future challenges. *Fire Safety Journal* 2017;91:41–55.
[14] Hu L, Kuang C, Zhong X, Ren F, Zhang X, Ding H. An experimental study on burning rate and flame tilt of optical-thin heptane pool fires in cross flows. *Proceedings of the Combustion Institute* 2017;36:3089–96.
[15] Lu Y, Huang X, Hu L, Fernandez-Pello C. The interaction between fuel inclination and

horizontal wind: Experimental study using thin wire. *Proceedings of the Combustion Institute* 2019;37:3809–16.
[16] Ji L, Wang J, Zhang W, Mao R, Hu G, Huang Z. Effect of confinement ratio on flame structure and blow-off characteristics of swirl flames. *Experimental Thermal and Fluid Science* 2022;135:110630.
[17] Wang Q, Liang X, Lu A, Wang B, Fujita O, Chung SH, et al. Blowout limits of inclined nonpremixed turbulent jet flames. *Proceedings of the Combustion Institute* 2022;000:1–10.
[18] Lu Y, Huang X, Hu L, Fernandez-Pello C. Concurrent Flame Spread and Blow-Off Over Horizontal Thin Electrical Wires. *Fire Technology* 2019;55:193–209.
[19] Ciardiello R, Skiba AW, Gordon RL, Mastorakos E. Experimental assessment of the lean blow-off in a fully premixed annular combustor. *Experimental Thermal and Fluid Science* 2020;112:109994.
[20] Loh HT, Fernandez-Pello AC, Fernandez-pello CA. Flow Assisted Flame Spread over Thermally Thin Fuels. *Fire Safety Science* 1986;1:65–74.
[21] Huang X, Link S, Rodriguez A, Thomsen M, Olson S, Ferkul P, et al. Transition from opposed flame spread to fuel regression and blow off: Effect of flow, atmosphere, and microgravity. *Proceedings of the Combustion Institute* 2019;37:4117–26.
[22] Chen Y, Fang J, Zhang X, Miao Y, Lin Y, Tu R, et al. Pool fire dynamics: Principles, models and recent advances. *Progress in Energy and Combustion Science* 2023;95:101070.
[23] Fu H, He C. Dynamics of coherent vortex rings in a successively generated turbulent pulsed jet. *Experimental Thermal and Fluid Science* 2022;136:110644.
[24] D.G. Akhmetov. Vortex Rings. vol. 3. Springer-Verlag Berlin Heidelberg; 2009.
[25] Panton RL. Impressible Flow. Wiley; 2013.
[26] Traveler C. Shape of the Aura: a Torus 2022.
[27] News J. Spitting smoke ring can make you the most philosophical cool-Interface News. 2016.
[28] Wikipedia. Vortex ring. 2022.
[29] Renard PH, Rolon JC, Thévenin D, Candel S. Investigations of heat release, extinction, and time evolution of the flame surface, for a nonpremixed flame interacting with a vortex. *Combustion and Flame* 1999;117:189–205.
[30] Pancharia P, Ramanan V, Sampath R, Chakravarthy SR. Effect of inlet flow turbulence on flame–vortex dynamics during thermo-acoustically induced flame flashback in a premixed dump combustor. *Experimental Thermal and Fluid Science* 2022;139:110733.
[31] Chiba Y, Torikai H, Ito A. Extinguishment Characteristics of a Jet Diffusion Flame with Inert-Gas Vortex Ring. In: Saito K, editor. Progress in Scale Modeling, vol. II, Springer; 2015, p. 115–25.
[32] Fu H, He C. An experimental study of coherent swirling vortex rings in a turbulent pulsed jet. *Experimental Thermal and Fluid Science* 2022;140:110762.
[33] Akhmetov DG, Lugovtsov BA, Tarasov VF. Extinguishing gas and oil well fires by means of vortex rings. *Combustion, Explosion, and Shock Waves* 1980;16:490–4.
[34] Giannuzzi PM, Hargather MJ, Doig GC. Explosive-driven shock wave and vortex ring interaction with a propane flame. *Shock Waves* 2016;26:851–7.
[35] Williams FA. Combustion Theory. 2nd ed. CRC Press; 1985.
[36] Drysdale D. An introduction to fire dynamics. 1998.
[37] Yershin SA. Theory of Vortex Rings. 2017.
[38] Niemann U, Seshadri K, Williams FA. Methane, ethane, and ethylene laminar counterflow diffusion flames at elevated pressures: Experimental and computational investigations up to 2.0MPa. *Combustion and Flame* 2014;161:138–46.
[39] Wang S, Huang X, Chen H, Liu N, Rein G. Ignition of low-density expandable polystyrene foam by a hot particle. *Combustion and Flame* 2015;162:4112–8.
[40] Xiong C, Liu Y, Xu C, Huang X. Extinguishing the dripping flame by acoustic wave. *Fire Safety Journal* 2021;120:103109.
[41] Jeon J, Shin D, Choi W, Kim SJ. Identification of the extinction mechanism of lean limit hydrogen flames based on Lewis number effect. *International Journal of Heat and Mass Transfer* 2021;174:121288.
[42] Vance FH, Shoshin Y, Van Oijen JA, De Goey LPH. Effect of Lewis number on premixed

laminar lean-limit flames stabilized on a bluff body. *Proceedings of the Combustion Institute* 2019;37:1663–72.
[43] Quintiere JG. Principles of fire behavior, Second Edition. 2016.
[44] Luton A, Ragab S, Telionis D. Interaction of spanwise vortices with a boundary layer. *Physics of Fluids* 1995;7:2757–65.
[45] Jiménez J. On the structure and control of near wall turbulence. *Physics of Fluids* 1994;6:944–53.
[46] Theodore LB. Fundamentals on Heat and Mass Transfer. 8th editio. Wiley; 2017.
[47] Ju X, Mizuno M, Matsuoka T, Yamazaki T, Kuwana K, Nakamura Y. Effect of circulation on flame heights over liquid fuel pools. *Combustion and Flame* 2022;246:112435.
[48] Yoshihara N, Ito A, Torikai H. Flame characteristics of small-scale pool fires under low gravity environments. *Proceedings of the Combustion Institute* 2013;34:2599–606.
[49] Tu R, Fang J, Zhang YM, Zhang J, Zeng Y. Effects of low air pressure on radiation-controlled rectangular ethanol and n-heptane pool fires. *Proceedings of the Combustion Institute* 2013;34:2591–8.
[50] NIST Chemistry WebBook 2022.